Journal of Hazardous Materials 213–214 (2012) 28–37

Contents lists available at SciVerse ScienceDirect

Journal of Hazardous Materials

journal homepage: www.elsevier.com/locate/jhazmat

Particulate matter (PM_{10}) exposure induces endothelial dysfunction and inflammation in rat brain

Lin Guo[a,1], Na Zhu[a,1], Zhen Guo[a], Guang-ke Li[a], Chu Chen[a], Nan Sang[a,*], Qing-chen Yao[b]

[a] College of Environment and Resource, Shanxi University, Taiyuan, Shanxi 030006, PR China
[b] Environmental Monitoring Central Station, Taiyuan, Shanxi 030002, PR China

ARTICLE INFO

Article history:
Received 5 April 2011
Received in revised form 5 December 2011
Accepted 11 January 2012
Available online 20 January 2012

Keywords:
PM_{10}
Brain
Endothelial dysfunction
Inflammatory response
Apoptosis

ABSTRACT

Epidemiological studies suggest that particulate matter (PM_{10}) inhalation was associated with adverse effects on brain-related health, however, existing experimental data lacked relevant evidences. In this study, we treated Wistar rats with PM_{10} at different concentrations (0.3, 1, 3 and 10 mg/kg body weight (bw)), and investigated endothelial dysfunction and inflammatory responses in the brain. The results indicate that mild pathological abnormal occurred after 15-day exposure (five times with 3 days each), followed by the changes of endothelial mediators (ET-1 and eNOS) and inflammatory markers (IL-1β, TNF-α, COX-2, iNOS and ICAM-1). Also, the sample up-regulated bax/bcl-2 ratio and p53 expression, and induced neuronal apoptosis. It implicates that PM_{10} exerted injuries to mammals' brain, and the mechanisms might be involved in endothelial dysfunction and inflammatory responses.

1. Introduction

There is mounting evidence that exposure to air pollution can cause stroke-related sickness and death [1,2], as well as brain damage, neurodegeneration [3–8], and many of these effects seem to be more strongly associated with particulate matters (PM). Paralleling this epidemiologic literature are intriguing findings from clinical experiments [9,10] and *in vivo* animal models [11,12], all pointing to the possibility that PM, especially inhalable particles (PM_{10}), can translocate from the upper respiratory tract to the central nervous system and the brain, and has been recorded in red blood cells (RBC), endothelial cells, and perivascular macrophages in olfactory bulb and frontal samples of humans and dogs [13]. However, experimental studies about its toxicological effects on the brain were scarce, and the specific mechanisms remained unclear.

A role for endothelial dysfunction and inflammation in various neurological disorders has recently been proposed on the basis of multiple lines of evidence [14]. The cerebrovascular endothelium plays a critical role in the regulation of normal vascular homeostasis, and perturbation of endothelial function is an important step in the pathogenesis [15]. Endothelial dysfunction is usually caused by altered production of vasoactive factors; especially, elevated ET-1 expression, the most potent vasoconstrictor, contributes to the reduction of blood flow, interruption of energy metabolism, and following injuries [16]. Also, the process is accompanied by dysregulation of the NO synthase pathways, which catalyze the production of NO from the amino acid L-arginine [17,18]. On the other hand, during the initiation and development of inflammatory, endothelial cells actively participate in this process by regulating leukocyte recruitment via enhancing the expression of proinflammatory enzymes, such as iNOS and cyclooxygenase-2 (COX-2), and the release of cytokines including interleukin-1β (IL-1β) and tumor necrosis factor-α (TNF-α), as well as the synthesis of adhesion molecules, such as intercellular adhesion molecule-1 (ICAM-1) [19]. Overproduction of these enzymes, cytokines, and adhesion molecules jointly causes circulating leukocytes to adhere to the endothelium, cross the vascular wall, enter the brain parenchyma, and eventually contribute to both necrotic and apoptotic neuronal death [19,20].

Endothelial dysfunction and inflammation do not play mutually independent roles, but are interrelated with each other. Therefore, we treated Wistar rats with PM_{10} at various concentrations (0.3, 1, 3 and 10 mg/kg body weight (bw)) to simulate the sub-acute exposure condition of people, and explored the histopathologic damages of cortex sections, and the expression of endothelial mediators (ET-1, eNOS) and inflammatory cytokines (IL-1β, TNF-α, COX-2, iNOS and ICAM-1). Following this, apoptosis-related gene expression (bax, bcl-2, p53) and subsequently neuronal apoptosis occurrence were investigated to clarify PM_{10}-induced injuries on the brain.

* Corresponding author.
E-mail address: sangnan_lgkcarl@yahoo.com.cn (N. Sang).
[1] These authors contributed equally to this work.

0304-3894/$ – see front matter © 2012 Elsevier B.V. All rights reserved.
doi:10.1016/j.jhazmat.2012.01.034

2. Materials and methods

2.1. PM_{10} sampling, chemical analysis and suspension preparation

2.1.1. PM_{10} sampling

The sampling site was located in Taiyuan city (112°57′E longitude, 37°73′N latitude), Shanxi Province, China. PM_{10} middle volume air sampler (TH-150C, Wuhan, China) was placed on the rooftop of a building about 10 m tall, and there were no large obstacles and no large pollution sources near the building. Airborne PM_{10} samples were collected on quartz filters from December 1, 2009 to January 30, 2010. The flow rate of the sampler was 100 L/min, and the sampling time was nominally 24 h with sampling starting at 9:00 a.m. During the sampling period, the average temperature was 2.32 °C and barometric pressure was 94.7 kPa.

2.1.2. Chemical analysis

PM_{10} mass concentration was determined by pre- and post-weighing the filters under controlled temperature and relative humidity. Inorganic ions, including ammonium (NH_4^+), nitrate (NO_3^-), sulfate (SO_4^{2-}), chlorine (Cl^-) and fluorine (F^-) were analyzed by ion chromatography. PM-bound metals and elements were assayed by inductively coupled plasma-mass spectrometry (ICP-MS). Organic carbon (OC) and element carbon (EC) were determined by thermal/optical reflection (TOR) assay, and polycyclic aromatic hydrocarbon (PAHs) were measured by gas chromatograph–mass spectrometer (GC–MS).

2.1.3. Preparing PM_{10} suspension and clarifying exposure concentration

The collected PM_{10} was transferred into aqueous suspension by 30 min soaking of PM_{10}-loaded filters in Milli-Q deionized water, followed by vortexing (5 min) and sonication (30 min). Prior to use, the dried sample was diluted with sterilized 0.9% physiological saline and swirled for 10 min. As a vehicle control for exposure experiments with resuspended PM_{10}, fresh sterile filters were sham extracted. Aqueous suspension was pooled and frozen at −20 °C.

As usually reported, respiratory volume of an adult rat is 200 ml/min, and respiratory volume for 3 days reaches 0.864 m^3. According to Grade III of PM_{10} in China (GB3095-1996), 0.25 mg/m^3, the amount of PM_{10} inhalation for 3 days is 0.216 mg. Therefore, PM_{10} exposure concentration for rat every 3 days should be 1.08 mg/kg bw. During the sampling period in the present study, PM_{10} concentration was 0.387 mg/m^3, and the highest and intermediate concentrations corresponded to the peak values reported in working environment reached 0.799 mg/m^3 [21]. Following this, different treatment concentrations, including 0.3, 1, 3 and 10 mg/kg, were used in the present study [22,23]. Although the experiments may be viewed as beyond the normal atmosphere encountered in the human environment, the following point must be taken into account. The animals were subjected to regular periods of extended exposure, with relief periods between protocols (i.e., 1 time/3 day, for 5 times, with 72 h between exposures). Also, the similar exposure concentration was reported in other studies.

2.2. Animals and treatment protocols

Male Wistar rats, weighing 190–210 g, were supplied by Experimental Animal Center, Academy of Military Medical Sciences of Chinese PLA (Beijing, China). The rats were routinely screened for common rat pathogens and housed in specific pathogen free facilities under standard conditions (24 ± 2 °C, 50 ± 5% humidity) with a 12-h light/dark cycle and food and water *ad libitum*.

The suspension was ultrasonicated for 15 min before intratracheal instillation, and the instillation was performed using a non-surgical intratracheal instillation method adapted [24,25]. Briefly, the animals were anesthetized by chloral hydrate. A ball tripped needle was maneuvered through the epiglottis, after which contact with the tracheal rings provides confirmation that the needle is, in fact, within the trachea. Then an injector with 0.5 ml physiological saline or PM_{10} suspension was inserted into the ball tripped needle. After gently instilled into the trachea, the animal was maintained in an upright position for 2 min to allow the fluid to drain into the respiratory tree. The rats were randomly divided into six equal groups of 6 animals each, and the experiment was carried out in duplicate. Four treatment groups were instilled PM_{10} suspension at different concentrations, and final exposure concentration reached 0.3, 1, 3 and 10 mg/kg bw, respectively. The control group was instilled with same amount of physiological saline, and the other special control group (vehicle group) was treated with same amount of suspension from extracts of "blank" filter. Instillation was performed five times with 3 days each.

When not being treated, the rats had free access to food and water. Decapitations 48 h after the last exposure, rats were killed. Cortex and lung were separated immediately after the brain was removed, and stored in prelabeled freezing tubes for quick freezing in liquid nitrogen and following by storage at −80 °C. The care and use of the animals reported in this study were approved by the Institutional Animal Care and Use Committee of Shanxi University.

2.3. Analytical methods

2.3.1. Hematoxylin–eosin (H&E) staining

The tissue was rapidly removed, washed for several times with 0.1 M phosphate buffer saline (PBS, pH 7.4), fixed in 10% formalin for 24 h at room temperature, dehydrated by graded ethanol and embedded in paraffin. Sections (5–6-μm-thick) were deparaffinized with xylene, stained with hematoxylin and eosin (HE), and observed by light microscopy with 400× magnification (Olympus, Japan).

2.3.2. Reverse transcription and real-time reverse transcription (RT)-PCR analysis

Total RNA was isolated from less than 100 mg of cortex and lung by using TRIzol Reagent (Invitrogen Life Technologies) according to the manufacturer's protocol. Total RNA was quantified by determination of optical density at 260 nm. First-strand complementary DNA (cDNA) was synthesized according to the manufacturer's instruction of reverse transcription kit (TaKaRa Biotechnology Co., Ltd., Dalian). The cDNA product was stored at −20 °C until use.

Each 20 μl PCR reaction contained 1 μl cDNA (5-fold dilution of original cDNA product), 2 μl PCR buffer, 3.5 mM $MgCl_2$, 0.2 mM of each dNTP, 500 nM each primer, 200 nM TaqMan probe and 1 U Taq DNA polymerase. The primers and probes were designed by using DnaStar and Beacon Design, and the sequences and cycling conditions were listed in Table 1. Reactions were run on a Rotor-Gene 3000 Real-Time Cycler (Corbett Research, Sydney, Australia).

Each treatment had six samples and each PCR reaction carried out in duplicate. In each PCR run, serial dilutions of known amounts of corresponding cDNA standard were included. To minimize inter-assay variability, the same dilution series of each gene-specific standard were run with samples in each experiment. The threshold cycle (Ct) was calculated by the Rotor-gene 6.0 software to indicate significant fluorescence signals above noise during the early cycles of amplification. Quantification of the samples by the software was calculated from Ct by interpolation from the standard curve to yield copy numbers for the target samples. The relative quantification of the expression of the target genes was measured using β-actin mRNA as an internal control. The copy number of target gene β-actin mRNA was measured in all samples.

Table 1
The sequences of primers and probes and cycling conditions.

Gene	Accession no.	Sequence	Temperature (t)				Cycles
			Initial denaturation	Denaturation	Annealing	Extended	
β-Actin	NM_017008	Sense: 5′-GCCCTAGACTTCGAGCAAGAG-3′ Antisense: 5′-AGCACTGTGTTGGCATAGAGGT-3′ TaqMan probe: 5′-FAM-CCACTGCCGCATCCTCTTCCTCCCT-TAMRA-3′	95 °C(3 min)	94 °C(20 s)	55 °C(20 s)	72 °C(20 s)	55
ET-1	NM_012548	Sense: 5′-AAGCGATCCTTGAAAGACTTACTTC-3′ Antisense: 5′-TGTGTATCAACTTCTGGTCTCTGTA-3′ TaqMan probe: 5′-FAM-ACCACAGACCAAGGGAACAGATGCC-TAMRA-3′	95 °C(3 min)	94 °C(20 s)	55 °C(20 s)	72 °C(20 s)	55
eNOS	NM_021838	Sense: 5′-CAGCGCCCACCCAGGAGAG-3′ Antisense: 5′-ATCGGCAGCCAAACACCAAAGTC-3′ TaqMan probe: 5′-FAM-CTGTAGCTGTGCTGGCATACAGAAC-TAMRA-3′	95 °C(3 min)	94 °C(20 s)	56 °C(20 s)	72 °C(20 s)	55
IL-1β	NM_031512	Sense: 5′-GCCTCAAGGGGAAGAATCTATACC-3′ Antisense: 5′-GGGAACTGTGCAGACTCAAACT-3′ TaqMan probe: 5′-FAM-TGATGAAAGACGGCACACCCACCCTTAMRA-3′	95 °C(3 min)	94 °C(20 s)	55 °C(20 s)	72 °C(20 s)	55
TNF-α	NM_012675	Sense: 5′-GCCGATTTGCCATTTCATACC-3′ Antisense: 5′-GGACTCCGTGATGTCTAAGTAC-3′ TaqMan probe: 5′-FAM-AGTCAGCCTCCTCTCCGCCATCAAG-TAMRA-3′	95 °C(3 min)	94 °C(20 s)	58 °C(20 s)	72 °C(20 s)	55
COX-2	NM_017232	Sense: 5′-AAATCGGGAGTTGGAATCACTTTC-3′ Antisense: 5′-CCATCGTTTAGGACAGAACATCAC-3′ TaqMan probe: 5′-FAM-TCCGCCACCTTCCTACGCCAGCA-TAMRA-3′	95 °C(3 min)	94 °C(20 s)	55 °C(20 s)	72 °C(20 s)	55
iNOS	NM_012611	Sense: 5′-CAGAAGCAGAATGTGACCATCAT-3′ Antisense: 5′-CGGAGGGACCAGCCAAATC-3′ TaqMan probe: 5′-FAM-ACCACCACACAGCCTCAGAGTCCTT-TAMRA-3′	95 °C(3 min)	94 °C(20 s)	55 °C(20 s)	72 °C(20 s)	55
ICAM-1	NM_012967	Sense: 5′-TTCAACCCGTGCCAGGC-3′ Antisense: 5′-GTTCGTCTTTCATCCAGTTAGTCT-3′ TaqMan probe: 5′-FAM-TCTGCTCCTGGTCCTGGTCGCCG-TAMRA-3′	95 °C(3 min)	94 °C(20 s)	58 °C(20 s)	72 °C(20 s)	55
bax	NM_017059	Sense: 5′-CCAAGAAGCTGAGCGAGTGTCTC-3′ Antisense: 5′-AGTTGCCATCAGCAAACATGTCA-3′ TaqMan probe: 5′-FAM-CCACCCGGAAGAAGACCTCTCGGGG-TAMRA-3′	95 °C(3 min)	94 °C(20 s)	55 °C(20 s)	72 °C(20 s)	55
bcl-2	NM_016993	Sense: 5′-GGAGCGTCAACAGGGAGATG-3′ Antisense: 5′-GATGCCGGTTCAGGTACTCAG-3′ TaqMan probe: 5′-FAM-TCCACAGAGCGATGTTGTCCACCA-TAMRA-3′	95 °C(3 min)	94 °C(20 s)	55 °C(20 s)	72 °C(20 s)	55
p53	NM_030989	Sense: 5′-CAGCTTTGAGGTTCGTGTTTGT-3′ Antisense: 5′-ATGCTCTTCTTTTTTGCGGAAA-3′ TaqMan probe: 5′-FAMCCTGTCCTGGGAGAGACCGTCGG-TAMRA-3′	95 °C(3 min)	94 °C(20 s)	55 °C(20 s)	72 °C(20 s)	55

2.3.3. Protein isolation and immunoblot analysis

Protein was extracted from cortex in ice-cold lysis buffer, and concentration was determined by bicinchoninic acid assay to ensure equal loading for assessment by sodium dodecyl sulfate-polyacrylamide gel electrophoresis (SDS-PAGE). Briefly, 50 μg total protein was separated by SDS-PAGE, transferred to a nitrocellulose membrane, and blocked with 5% nonfat milk. Blocked membranes were incubated in either rabbit polyclonal antibodies specific for rat ET-1, eNOS, COX-2, iNOS and ICAM-1 (Beijing Biosynthesis Biotechnology Co., Ltd.), or mouse monoclonal antibodies for β-actin (Oncogene, USA) at a concentration of 1:100 (for ET-1, eNOS, COX-2, iNOS and ICAM-1), or 1:5000 (for β-actin) at 4 °C overnight. Exposure to fluorescently labeled secondary antibody (1: 2000) (IRDye 800CW Goat anti-Rabbit IgG (H + L), LI-COR) was followed by scanning and detecting with LI-COR Odyssey® Infrared Fluorescent.

2.3.4. Determination of cytokine level

The tissue was weighed and homogenized in ice-cold 0.9% NaCl and centrifuged for 10 min at 3000 rpm. Cytokine (IL-1β and TNF-α) levels in the supernatant were measured with commercially ELISA kits (Westang Company, China), according to the manufacture instruction.

2.3.5. TUNEL assay

Tissue section of rat brain was fixed with 4% paraformaldehyde and embedded in paraffin, and then processed for the terminal deoxynucleotidyl transferase mediated dUTP nick end labeling (TUNEL) assay according to manufacture instructions (Apoptag® Plus Peroxidase in situ Apoptosis Detection Kit, Roche Company, Purchase, Shanghai). After developed with diaminobenzidine (DAB) substrate, slides were also counterstained with hematoxylin, and then examined for evidence of apoptosis. Cell with bright brunette nucleus was considered to be TUNEL-positive cell.

2.4. Data analysis

Data were presented as mean ± SE. Unless stated otherwise, analysis of variance (ANOVA) was applied for between-group statistical comparison using StatView Software. Results presented were representative, and those with p-values < 0.05 were considered significant.

3. Results

3.1. Analysis of PM_{10} chemical characteristics

The daily average sampling weight of PM_{10} was 0.0557 g, and the concentration was 0.387 mg/m^3. As shown in Table 2, inorganic ions in the PM_{10} sample mainly included NH_4^+, NO_3^-, SO_4^{2-}, Cl^- and F^-, and elements were consisted of Na, K, Mg, P, Ca, Fe, Al. The data from ICP-MS and GC–MS indicate that the heavy metal Mn, Zn, As, Cu, Ni, Cr, Cd, Co, Pb, Ba, Sc and Sb were detected, and 17 PAHs were found. Also, we analyzed EC and OC, and the values reached 38.130 and 85.338 μg/m^3, respectively.

3.2. Effects of PM_{10} on brain histology and apoptosis

Representative H&E staining images were shown in Fig. 1A–E. No histopathological abnormalities were observed in control and vehicle group animals (data not shown). After different concentration PM_{10} exposure, astrocytes occurred around neurons, following with a small amount of eosinophilic cytoplasm. Numerous glial nuclei surrounded with shrunken cytoplasmic bodies were

Table 2
The chemical characteristics of PM_{10} sample.

Elements (μg/m³)		Inorganic ions (μg/m³)		Heavy metal (ng/m³)		Polycyclic aromatic hydrocarbon (PAHs, ng/m³)	
Na	2.684	NH_4^+	6.924	Mn	0.403	Acenaphthylene (ANY)	0.822
K	5.085	NO_3^-	19.129	Zn	1.163	Acenaphthene (ANA)	0.136
Mg	14.748	SO_4^{2-}	75.155	As	0.413	Fluorene (FLU)	1.142
P	1.222	Cl^-	46.430	Cu	0.587	Benzo(g,hi)perylene (BPE)	54.381
Ca	96.635	F^-	0.600	Ni	0.026	Indeno(1,2,3-cd)pyrene (IPY)	41.407
Fe	9.679			Cr	0.044	Dibenzo(a,h)anthracene (DBA)	18.828
Al	17.490			Cd	0.007	Benzo(b)fluoranthene (BbF)	82.352
OC	85.338			Co	0.009	Coronene (COR)	33.375
EC	38.130			Pb	0.693	Phenanthrene (PHE)	27.977
				Ba	2.730	Anthracene (ANT)	7.310
				Sc	0.020	Fluoranthene (FLT)	78.284
				Sb	0.184	Benzo(a)anthracene (BaA)	66.592
						Chrysene (CHR)	67.184
						Pyrene (PYR)	87.524
						Benzo(a)pyrene (BaP)	41.678
						Benzo(e)pyrene (BeP)	32.968
						Benzo(k)fluoranthene (BKF)	13.939

observed. Moreover, large pyramidal neurons were particularly affected while neuronal cell loss was remarkable.

Following the qualitative description, TUNEL staining was applied to quantificate the changes. As shown in Fig. 2A–F, little specific staining occurred in control and vehicle group (5.6 ± 0.51% and 5.5 ± 0.73% ($p > 0.05$ *vs* control) immunoreactive cells), and the number of TUNEL-positive neurons increased in a concentration-dependent manner (6.6 ± 1.12%, 10.6 ± 0.51%, 17.2 ± 0.92% and 22.4 ± 1.29% immunoreactive neurons at 0.3, 1, 3 and 10 mg/kg bw, respectively).

3.3. Effects of PM_{10} on expression of endothelial mediators in the cortex

ET-1 mRNA level varied with treatment concentration in a bell-shape manner, and reached peak value at 1 mg/kg bw (2.24-fold of control) (Fig. 3A_1). Whereas, ET-1 protein increased with a concentration-dependent property, and the statistical difference occurred at all treated concentrations (1.55-, 1.62-, 1.67- and 1.70-fold of control for 0.3, 1, 3 and 10 mg/kg bw, respectively) (Fig. 3A_2).

Conversely, eNOS mRNA and protein expression decreased after PM_{10} exposure with a concentration-dependent property (Fig. 3B), and reached 0.74-, 0.57-, and 0.13-fold of control for mRNA, and 0.72-, 0.59-, and 0.72-fold of control for protein at 1, 3 and 10 mg/kg bw.

3.4. Effects of PM_{10} on expression of inflammatory markers in the cortex

PM_{10} exposure tended to increase IL-1β expression at mRNA and protein levels at all concentrations tested, and statistical differences were observed at higher concentrations (for mRNA, 1.90-,

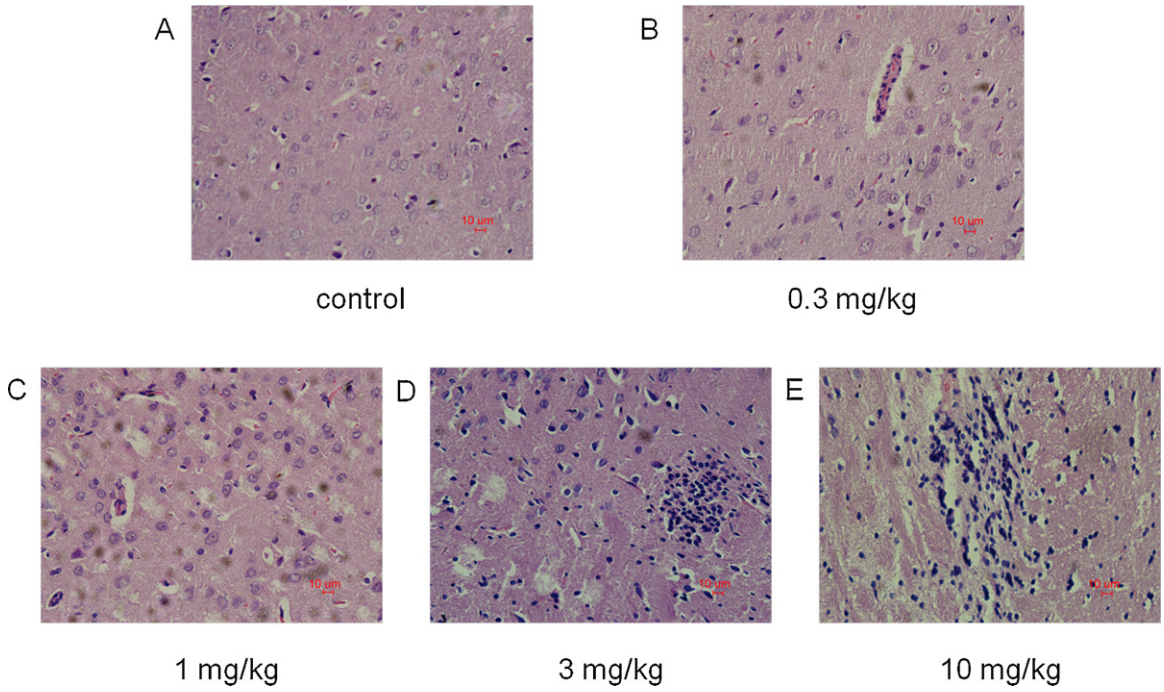

Fig. 1. The morphological characteristics in the brain of rats from control (A), 0.3 mg/kg (B), 1 mg/kg (C), 3 mg/kg (D) and 10 mg/kg (E). The brain from different treatment group was rapidly removed, washed for several times with 0.01 M PBS (pH 7.4), fixed in 10% formalin for 24 h at room temperature, dehydrated by graded ethanol and embedded in paraffin. Sections (5- or 6-μm-thick) were deparaffinized with xylene, stained with hematoxylin and eosin, and observed by light microscopy with 400× magnification. The control reported in the figure represented normal control. The control group was instilled with same amount of physiological saline, and instillation was performed five times with 3 days each. Bar = 10 μm.

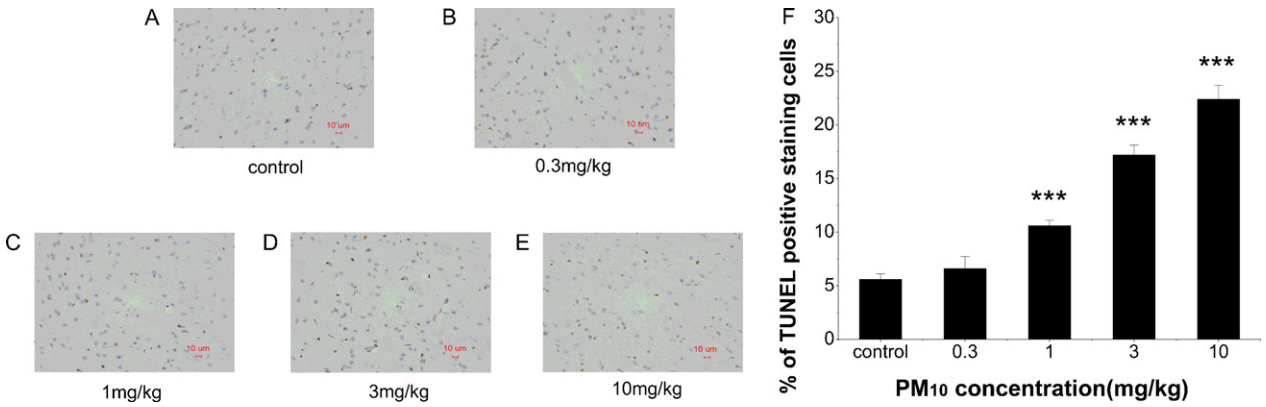

Fig. 2. TUNEL staining in the brain of rats from control (A), 0.3 mg/kg (B), 1 mg/kg (C), 3 mg/kg (D), 10 mg/kg (E), and average percentages of TUNEL positive staining cells (F). Tissue section of rat brain was fixed with 4% paraformaldehyde and embedded in paraffin, and then processed for the terminal deoxynucleotidyl transferase mediated dUTP nick end labeling (TUNEL) assay according to manufacturer's instructions. After developed with diaminobenzidine (DAB) substrate, slides were also counterstained with hematoxylin, and observed by light microscopy with 400× magnification. The control reported in the figure represented normal control, and no statistical difference was observed between normal control and vehicle control group ($p > 0.05$, $n = 6$). Bar = 10 μm.

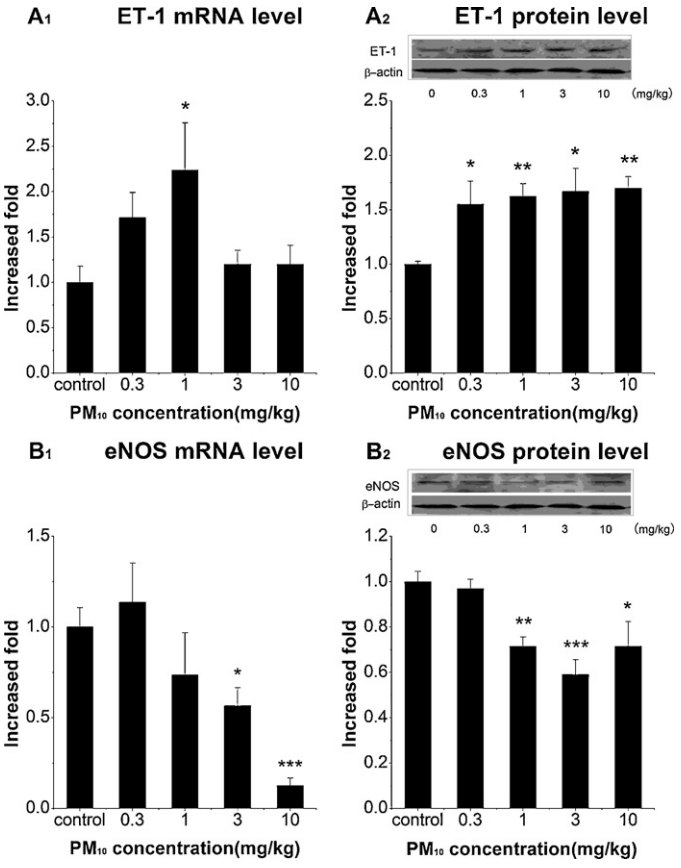

Fig. 3. Effects of PM_{10} exposure on ET-1 (A_1 and A_2) and eNOS (B_1 and B_2) mRNA and protein expression in rat brain. Male Wistar rats were instilled PM_{10} suspension at different concentrations, and final exposure concentration reached about 0.3, 1, 3 and 10 mg/kg bw, respectively. The control group was instilled with same amount of physiological saline, and the other special control group (vehicle group) was treated with same amount of suspension from extracts of "blank" filter. The rats were instilled for five times with 3 days each. Each treatment had six samples and each PCR reaction carried out in duplicate. Value in each treated group was expressed as a fold increase compared to mean value in control group, which has been ascribed as an arbitrary value of 1. The control reported in the figure represented normal control, and no statistical difference was observed between normal control and vehicle control group ($p > 0.05$, $n = 6$). Data are expressed as means ± SE ($n = 6$); $^{*}p < 0.05$, $^{**}p < 0.01$, $^{***}p < 0.001$ *vs* negative control.

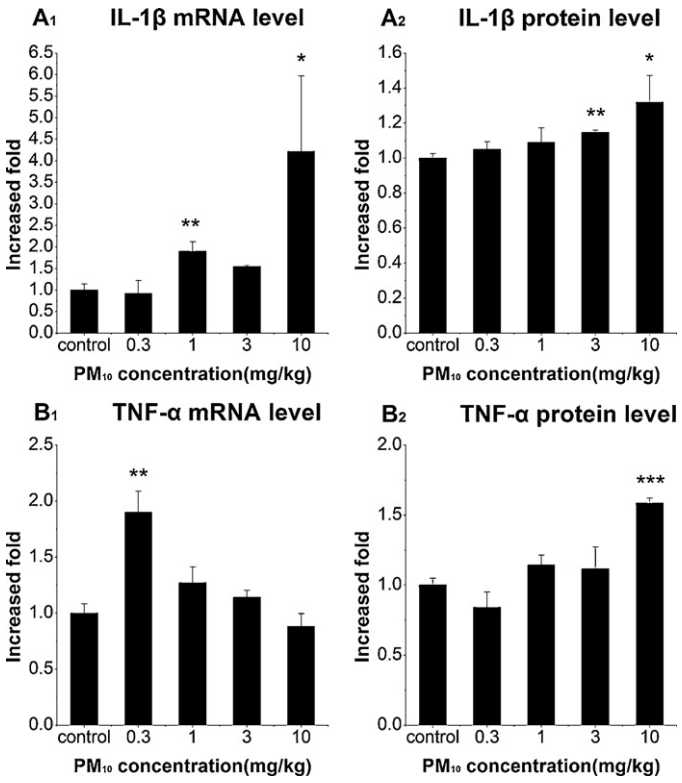

Fig. 4. Effects of PM_{10} exposure on IL-1β (A_1 and A_2), TNF-α (B_1 and B_2) mRNA and protein expression in rat brain. Male Wistar rats were instilled PM_{10} suspension at different concentrations, and final exposure concentration reached about 0.3, 1, 3 and 10 mg/kg bw, respectively. The control group was instilled with same amount of physiological saline, and the other special control group (vehicle group) was treated with same amount of suspension from extracts of "blank" filter. The rats were instilled for five times with 3 days each. Each treatment had six samples and each PCR and ELISA reaction carried out in duplicate. Value in each treated group was expressed as a fold increase compared to mean value in control group, which has been ascribed as an arbitrary value of 1. The control reported in the figure represented normal control, and no statistical difference was observed between normal control and vehicle control group ($p > 0.05$, $n = 6$). Data are expressed as means ± SE ($n = 6$); $^{*}p < 0.05$, $^{**}p < 0.01$, $^{***}p < 0.001$ *vs* negative control.

1.55- and 4.22-fold of control at 1, 3 and 10 mg/kg bw; for protein, 1.15- and 1.32-fold of control at 3 and 10 mg/kg bw) (Fig. 4A). TNF-α mRNA expression followed a bell-shape concentration-response, with a peak value occurring at 0.3 mg/kg bw (1.90-fold of control). Whereas, TNF-α protein increased with treatment concentration, and statistical difference was observed after 10 mg/kg bw (1.59-fold of control) (Fig. 4B).

COX-2 mRNA level varied with treatment concentration in a bell-shape manner (Fig. 5A$_1$). The value reached peak value at 1 mg/kg bw (2.23-fold of control) and then decreased with the increase of concentration. However, COX-2 protein expression was continuously up, and the statistical difference occurred at 1, 3 and 10 mg/kg (1.28-, 1.38- and 1.26-fold of control). PM_{10} exposure significantly enhanced iNOS mRNA and protein expression with a concentration-dependent property, and statistical difference occurred at all concentrations tested (Fig. 5B). Also, PM_{10} tended to increase ICAM-1 expression at mRNA and protein levels at all concentrations tested, and statistical differences were observed at higher concentrations (for mRNA, 1.30-, 1.44-, 1.51- and 1.91-fold of control at 0.3, 1, 3 and 10 mg/kg bw; for protein, 1.33-, 1.38- and 1.50-fold of control at 1, 3 and 10 mg/kg bw) (Fig. 5C).

3.5. Effects of PM_{10} on expression of apoptosis-related genes in the cortex

To clarify the sequent injuries of PM_{10} on the brain, we further investigated the expression of apoptosis-related genes (Fig. 6). PM_{10} exposure tended to increase bax expression at mRNA and protein levels at all concentrations tested, and statistical differences were observed at 1, 3 and 10 mg/kg bw. The sample tended to decrease bcl-2 expression, but no statistical difference was found. Whereas, the ratio of bax to bcl-2 mRNA/protein elevated with the increase of exposure concentration, and statistical differences occurred at all tested concentrations. Also, the sample elevated p53 mRNA and protein expression in a concentration-dependent manner, and the significant difference occurred at 3 and 10 mg/kg bw.

3.6. Effects of PM_{10} on expression of endothelial and inflammatory marker genes in the lung

As shown in Fig. 7, ET-1 mRNA level increased with a concentration-dependent property, and the statistical difference occurred at the two treated concentrations (1.76- and 2.79-fold of control for 0.3 and 3 mg/kg bw, respectively). IL-1β and ICAM-1 expression at mRNA increased with treatment concentration, and statistical difference was observed at 3 mg/kg bw (1.27-fold and 2.45-fold of control, respectively). TNF-α mRNA level tended to increase with treatment concentration, and no statistical difference was observed at present exposure levels.

4. Discussion

Air pollution is a complex mixture of gases and particulate matter. In some urban areas, the air quality is so poor that the threshold considered 'safe' is consistently surpassed due to the combustion of fossil fuels. In such environments, exposure to ambient air pollution and the possibility of adverse human health effects is a realistic cause for concern. While the connection between exposure to particulate matter and harmful cardiopulmonary effects has been reasonably well established [26,27], there is growing evidence that the central neuronal system (CNS) may be another target and PM may be associated with cerebrovascular and neurodegenerative diseases [3,15,28]. In the present study we demonstrate that mild pathological abnormal occurred in the brain after PM_{10} exposure in heating season, followed by the changes of endothelial mediators

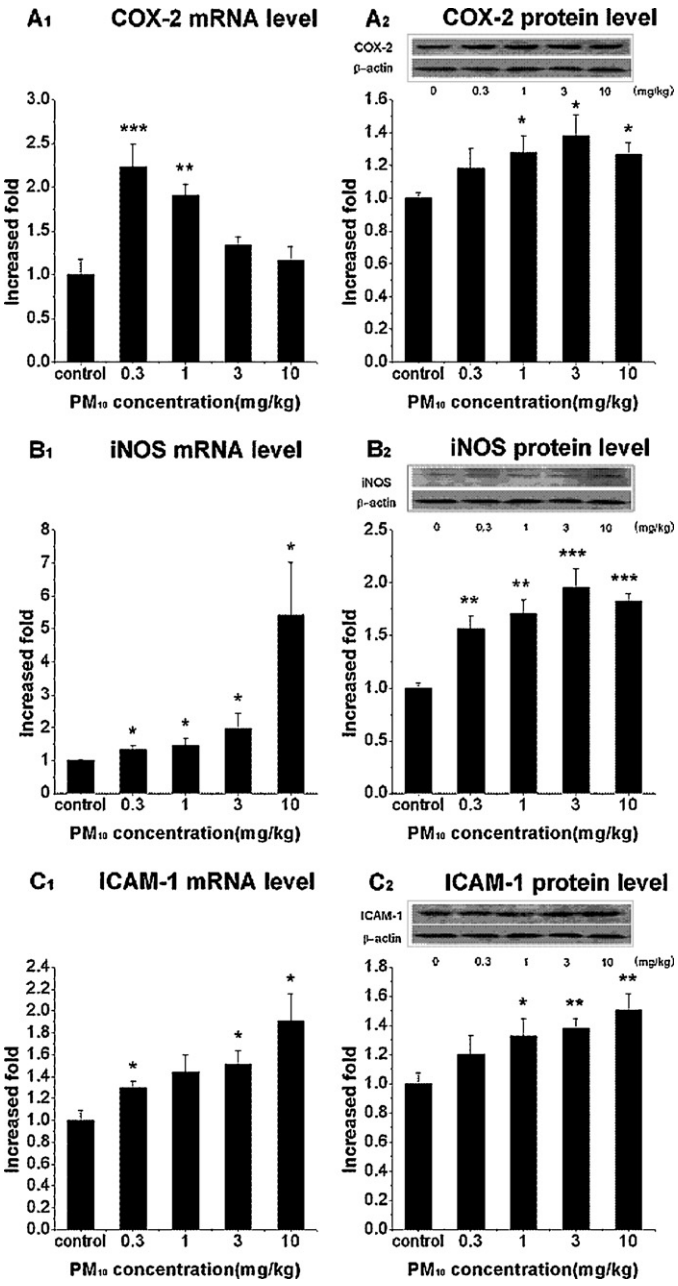

Fig. 5. Effects of PM_{10} exposure on COX-2 (A_1 and A_2), iNOS (B_1 and B_2), ICAM-1 (C_1 and C_2) mRNA and protein expression in rat brain. Male Wistar rats were instilled PM_{10} suspension at different concentrations, and final exposure concentration reached about 0.3, 1, 3 and 10 mg/kg bw, respectively. The control group was instilled with same amount of physiological saline, and the other special control group (vehicle group) was treated with same amount of suspension from extracts of "blank" filter. The rats were instilled for five times with 3 days each. Each treatment had six samples and each PCR and ELISA reaction carried out in duplicate. Value in each treated group was expressed as a fold increase compared to mean value in control group, which has been ascribed as an arbitrary value of 1. The control reported in the figure represented normal control, and no statistical difference was observed between normal control and vehicle control group ($p > 0.05$, $n = 6$). Data are expressed as means ± SE ($n = 6$); $^*p < 0.05$, $^{**}p < 0.01$, $^{***}p < 0.001$ *vs* negative control.

(ET-1 and eNOS) and inflammatory markers, (IL-1β, TNF-α, iNOS, COX-2 and ICAM-1). Also, the sample up-regulated bax/bcl-2 ratio and p53 expression, and induced neuronal apoptosis. However, the sample suspension from the special control group, which was treated with extracts of "blank" filter, did not affect the expression of endothelial dysfunction mediators and inflammatory markers, and no statistical difference was observed between normal control

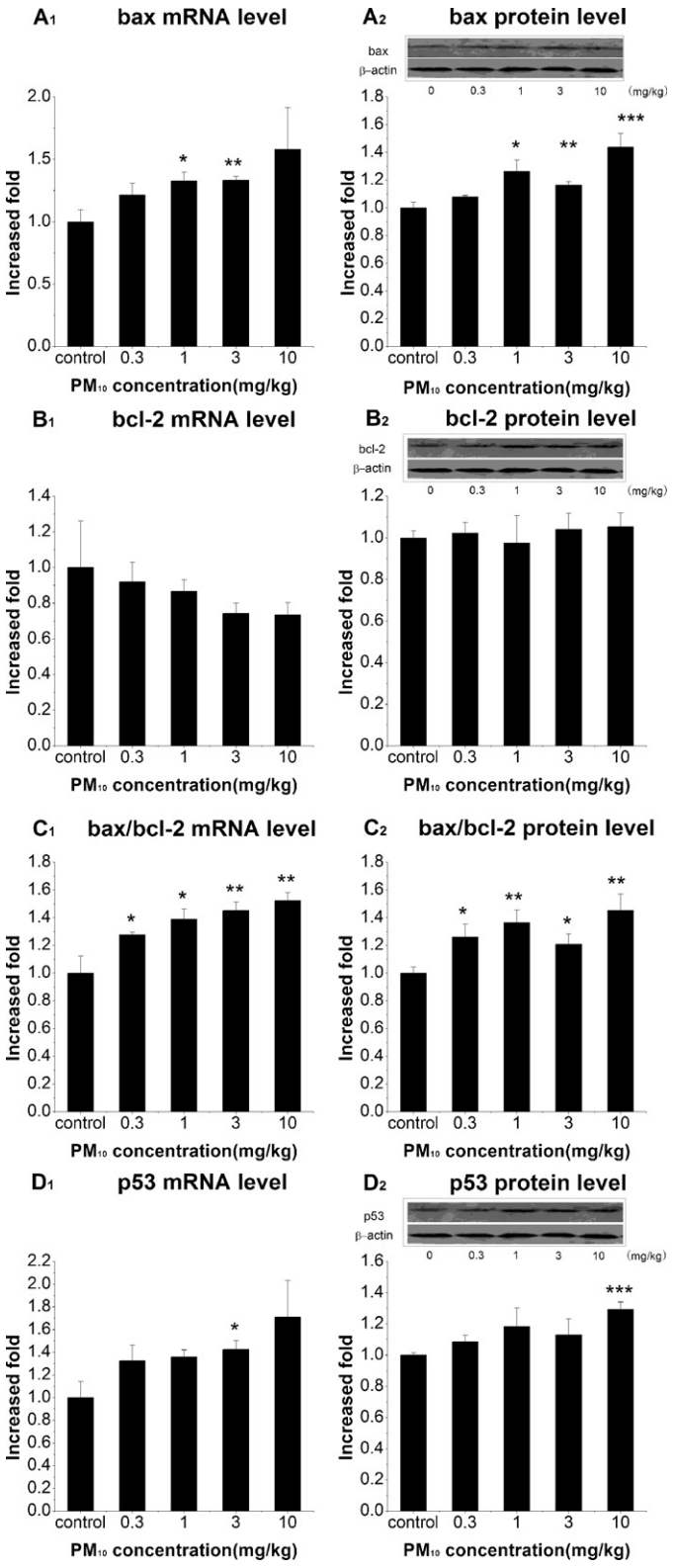

Fig. 6. Effects of PM_{10} exposure on bax (A_1 and A_2), bcl-2 (B_1 and B_2), bax/bcl-2 (C_1 and C_2) and p53 (D_1 and D_2) mRNA and protein expression in rat brain. Male Wistar rats were instilled PM_{10} suspension at different concentrations, and final exposure concentration reached about 0.3, 1, 3 and 10 mg/kg bw, respectively. The control group was instilled with same amount of physiological saline, and the other special control group (vehicle group) was treated with same amount of suspension from extracts of "blank" filter. The rats were instilled for five times with 3 days each. Each treatment had six samples and each PCR carried out in duplicate. Value in each treated group was expressed as a fold increase compared to mean value in control group, which has been ascribed as an arbitrary value of 1. The control and special control group (data not shown). It implicates that PM_{10} exerted injuries to mammals' brain, and the mechanisms might be involved in endothelial dysfunction and inflammatory responses.

Endothelins are potent vasoactive peptides upregulated in a number of disorders involving endothelial dysfunction, secondary to endothelial nitric oxide synthase-derived nitric oxide inhibition and over-expression of ET-1 [29]. NO is the most important vasodilator, while ET-1 is one of the most potent endogenous vasoconstrictors. The critical balance of NO and ET-1 is vital in normal physiology and is disrupted in pathologic conditions [30]. After PM_{10} exposure, ET-1 expression increased and eNOS level decreased with a concentration-dependent property, and the statistical difference occurred at higher concentrations. As a vasoconstrictor, ET-1 mediates a host of responses including endothelial dysfunction, vasomotor contraction, leukocyte activation and cellular proliferation, all of that eventually cause injuries [31]. ET-1 participates in the initiation of gliosis [32,33], a feature of neurodegeneration [34,35]. Elevated plasma ET-1 levels may penetrate the brain either by transport or leakage across a permeabilized BBB. ET-1 can also inhibit NO production through regulating the expression of NO synthases [36], which may explain the decline of eNOS expression after high concentration PM_{10} exposure. Considering the close relationship between ET-1 and eNOS, we suggest that ET-1 and eNOS were two key factors in the development of PM_{10}-mediated brain endothelial injury.

Accumulating experimental studies show that air pollution-induced neuronal disorders are associated with a marked inflammatory reaction, and proinflammatory enzymes including iNOS and COX-2 play an important role among the process. In general, cytokines, produced by macrophages, endothelial cells, astrocytes, fibroblasts, and neurons, are likely to contribute to the expression. Principal among the factors are IL-1β and TNF-α, two typical pro-inflammatory cytokines and form an important part of inflammatory response, which enhance the permeability of endothelial cells and display important physiological activities in the initiation and development of the host response to brain injuries [19,37]. In addition to attracting leukocytes into damage sites, cytokines also stimulate the synthesis of adhesion molecules, such as ICAM-1, on leukocytes and endothelial cells as well as other cell types to promote the infiltration of leukocytes to the brain through the endothelial wall [38,39]. In the present study, we first measured IL-1β and TNF-α release, and found that the two typical pro-inflammatory cytokines was stimulated by PM_{10} exposure and it implicated the initiation of inflammatory process. Following this, induced excessive COX-2, iNOS and ICAM-1 expression promoted blood-borne inflammatory cell adherence and infiltration. Consequently, leukocytes exacerbated brain injury by physically obstructing capillaries and reducing blood flow and/or by migrating into the brain parenchyma and releasing cytotoxic products, which implicates the occurrence and development of injuries in rat brains via inflammatory mechanism after PM_{10} exposure.

Interestingly, we observed the disagreement of the mRNA and protein expression for the inflammatory markers. Usually, the timing for mRNA expression and protein is different, and the expression of mRNA is earlier than that of protein. It was probably due to PM_{10} at various concentrations stimulated mRNA expression at different time point, and the time to induce the elevation of mRNA level was shorter at higher concentrations than that at lower concentrations. Therefore, the protein level followed a similar concentration-course as the corresponding mRNA at lower concentrations, but did not follow a similar course as the corresponding

reported in the figure represented normal control, and no statistical difference was observed between normal control and vehicle control group ($p > 0.05$, $n = 6$). Data are expressed as means ± SE ($n = 6$); $^{*}p < 0.05$, $^{**}p < 0.01$, $^{***}p < 0.001$ *vs* negative control.

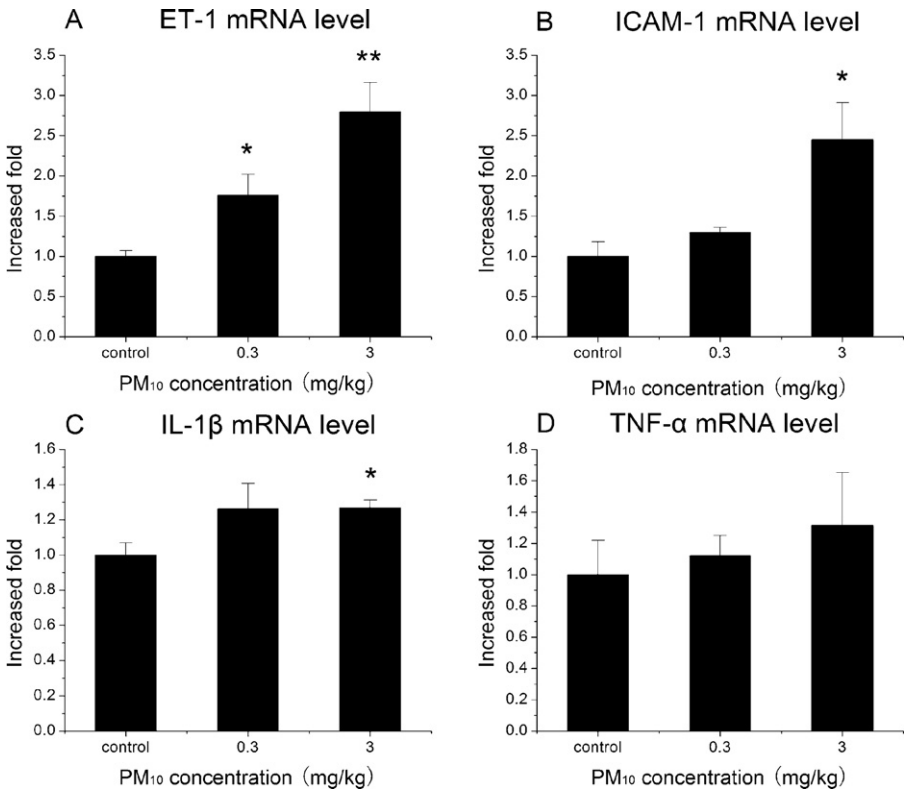

Fig. 7. Effects of PM_{10} exposure on ET-1 (A), ICAM-1 (B), IL-1β (C) and TNF-α (D) mRNA in rat lung. Male Wistar rats were instilled PM_{10} suspension at different concentrations, and final exposure concentration reached about 0.3 and 3 mg/kg bw, respectively. The control group was instilled with same amount of physiological saline. The rats were instilled for five times with 3 days each. Each treatment had six samples and each PCR reaction carried out in duplicate. Value in each treated group was expressed as a fold increase compared to mean value in control group, which has been ascribed as an arbitrary value of 1. The control reported in the figure represented normal control, and no statistical difference was observed between normal control and vehicle control group ($p > 0.05$, $n = 6$). Data are expressed as means ± SE ($n = 6$); $^{*}p < 0.05$, $^{**}p < 0.01$, $^{***}p < 0.001$ *vs* negative control.

mRNA at higher concentrations, where the maximal mRNA expression was earlier than that of protein expression.

Neuronal apoptosis is implicated in the pathogenesis of an increasing number of diseases which can be initiated by diverse signals (such as oxidative stress and inflammation) and executed via different biochemical pathways [40]. In the present study, PM_{10}-induced apoptosis was mediated by the p53-dependent mitochondrial apoptotic pathway as indicated by increased expression of p53 as well as its downstream target bax/bcl-2 ratio. Also, TUNEL staining assay presented increased apoptotic neuron density and confirmed the results.

Considering the PM_{10} sample used in the present study was collected during heating season from a coal-combustion polluted city, we further provided extra chemical characteristics data on the sample, including heavy metals, organic and elemental carbon, and PAHs. Inorganic ions in the PM_{10} sample included NH_4^+, NO_3^-, SO_4^{2-}, Cl^- and F^-, and SO_4^{2-} reached higher level, which suggesting seriously SO_2 exhausting from heating process during winter and industrial coal-combustion [41]. Among heavy metals, Mn, As, Pb, Ba and Sb, important contributors of heavy metal releasing from coal-combustion [42], were richer than others. Also, 17 priority PAHs from coal-combustion process were detected [43], and Benzo(g,hi)perylene (BPE), Indeno (1,2,3-cd)pyrene (IPY), Benzo(b)fluoranthene (BbF), Coronene (COR), Fluoranthene (FLT), Benzo(a)anthracene (BaA), Chrysene (CHR), Pyrene (PYR) and Benzo(a)pyrene (Bap) showed higher polluting loads. To clarify the source, we analyzed EC and OC, and the value of OC/EC implied that the PM sample mainly came from coal-combustion process [44]. It substantiates the notion that the PM_{10}-bound pollutants resulting from coal-combustion played important role on the injuries of the brain, and PM exposure in coal-combustion atmospheric environment might contribute to the development and progression of neuronal dysfunction.

Since the primary sites of PM_{10} impact are lungs, we further provided some data on lung toxicity of the PM_{10} sample to interpret whether the effects on the brain derive from either particle translocation or systemic inflammatory events promoted by lung cells. Stimulated expression of lung endothelial mediators and inflammatory markers from the present PM_{10} treatment was consistent with previous literatures that exposures to particulate matter have been associated with respiratory tract inflammation, disruption of the nasal respiratory and olfactory barriers, systemic inflammation, production of mediators of inflammation capable of reaching the brain and systemic circulation of particulate matter [5,14]. The olfactory pathway provides a route by which metals and other toxicants that come into contact with the olfactory epithelium can enter the central nervous system without the interference of the blood–brain-barrier. On the other hand, inflammatory mediators, produced in the respiratory tract as a consequence of chronic pollutant-induced epithelial and endothelial injury, and released into the circulation could activate brain endothelium and cross the blood–brain barrier (BBB) [7,45]. Respiratory tract endothelial and epithelial injury elicits the production and release into the circulation of IL-6, IL-1β, tumor necrosis factor-α (TNF-α) and GM-CSF [46–48]. Brain blood vessels express receptors for TNF-α, IL-1β, and IL-6 [49,50]. TNF-α and IL-1β can evoke expression of inflammatory mediator genes, such as cyclooxygenase-2 (COX2) [51] and inducible nitric oxide synthase (iNOS) within brain capillary endothelium [52,53]. Systemic cytokines could also affect the central nervous system (CNS) via sensory nerves such as the vagus. Alternatively, the carbon core of fine and ultrafine PM and PM-associated chemicals, including combustion-derived metals, such

as vanadium and nickel, and polyaromatic hydrocarbons, might evoke brain inflammation by acting directly on the brain. Controlled exposures of rats to particles or metals suggest that the PM or PM components accumulate in the olfactory bulb [54,55], and the trigeminal pathway can transport neurotoxins to the brain [56]. Thus, PM may reach the brain through olfactory receptor neurons and the trigeminal nerves. Therefore, the observed effects on the brain in the present study derive from particle translocation and systemic inflammatory events promoted by lung cells.

5. Conclusion

In this study, we treated Wistar rats with PM_{10} at different concentrations (0.3, 1, 3 and 10 mg/kg body weight), and investigated endothelial dysfunction and inflammatory responses in the brain. The results indicate that mild pathological abnormal occurred after 15-day exposure (1 time per 3 days), followed by the changes of endothelial mediators (ET-1 and eNOS) and inflammatory markers, (IL-1β, TNF-α, COX-2, iNOS and ICAM-1). Also, the sample up-regulated bax/bcl-2 ratio and p53 expression, and induced neuronal apoptosis. It implicates that PM_{10} exerted injuries to mammals' brain, and the mechanisms might be involved in endothelial dysfunction and inflammatory responses.

Acknowledgments

This study was supported by National Natural Science Foundation of P. R. China (NSFC, No. 20607013, 20877050, 20977060), Natural Science Foundation of Shanxi Province (No. 2009011049-3, 2009011046, 20051043), Specialized Research Fund for the Doctoral Program of Higher Education (SRFDP, No. 20091401110002), Program for New Century Excellent Talents in University (No. NCET-10-0927), Research Project Supported by Shanxi Scholarship Council of China (No. 2011-013), and Program for the Top Young Academic Leaders of Higher Learning Institutions of Shanxi.

References

[1] Y.C. Hong, J.T. Lee, H. Kim, E.H. Ha, J. Schwartz, D.C. Christiani, Effects of air pollutants on acute stroke mortality, Environ. Health Perspect. 110 (2002) 187–191.
[2] R. Maheswaran, T. Pearson, M.J. Campbell, R.P. Haining, C.W. McLeod, N. Smeeton, C.D. Wolfe, A protocol for investigation of the effects of outdoor air pollution on stroke incidence, phenotypes and survival using the South London Stroke Register, Int. J. Health Geogr. 5 (2006) 1–10.
[3] L. Calderón-Garcidueñas, R.R. Maronpot, R. Torres-Jardon, C. Henríquez-Roldán, R. Schoonhoven, H. Acuña-Ayala, A. Villarreal-Calderón, J. Nakamura, R. Fernando, W. Reed, B. Azzarelli, J.A. Swenberg, DNA damage in nasal and brain tissues of canines exposed to air pollutants is associated with evidence of chronic brain inflammation and neurodegeneration, Toxicol. Pathol. 31 (2003) 524–538.
[4] L. Calderón-Garcidueñas, W. Reed, R.R. Maronpot, C. Henríquez-Roldán, R. Delgado-Chavez, A. Calderón-Garcidueñas, I. Dragustinovis, M. Franco-Lira, M. Aragón-Flores, A.C. Solt, M. Altenburg, R. Torres-Jardón, J.A. Swenberg, Brain inflammation and Alzheimer's-like pathology in individuals exposed to severe air pollution, Toxicol. Pathol. 32 (2004) 650–658.
[5] L. Calderón-Garcidueñas, M. Franco-Lira, R. Torres-Jardón, C. Henriquez-Roldán, G. Barragán-Mejía, G. Valencia-Salazar, A. Gonzalez-Maciel, R. Reynoso-Robles, R. Villarreal-Calderon, W. Reed, Pediatric respiratory and systemic effects of chronic air pollution exposure: nose, lung, heart and brain pathology, Toxicol. Pathol. 35 (2007) 154–162.
[6] L. Calderón-Garcidueñas, A. Solt, M. Franco-Lira, C. Henríquez-Roldán, R. Torres-Jardón, B. Nuse, L. Herritt, R. Villarreal-Calderon, N. Osnaya, I. Stone, R. Garcia, D.M. Brooks, A. Gonzalez-Maciel, R. Reynoso-Robles, R. Delgado-Chavez, W. Reed, Long-term air pollution exposure is associated with neuroinflammation, an altered innate immune response, disruption of the blood–brain barrier, ultrafine particle deposition, and accumulation of amyloid beta 42 and alpha synuclein in children and young adults, Toxicol. Pathol. 36 (2008) 289–310.
[7] A. Peters, B. Veronesi, L. Calderón-Garcidueñas, P. Gehr, L. Chi Chen, M. Geiser, W. Reed, B. Rothen-Rutishauser, S. Schurch, H. Schulz, Translocation and potential neurological effects of fine and ultrafine particles a critical update, Part. Fibre Toxicol. 3 (2006) 1–13.
[8] S.M. Mohankumar, A. Campbell, M. Block, B. Veronesi, Particulate matter, oxidative stress and neurotoxicity, Neurotoxicology 29 (2008) 479–488.
[9] R.D. Brook, J.R. Brook, B. Urch, R. Vincent, S. Rajagopalan, F. Silverman, Inhalation of fine particulate air pollution and ozone causes acute arterial vasoconstriction in healthy adults, Circulation 105 (2002) 1534–1536.
[10] K.W. Rundell, J.R. Hoffman, R. Caviston, R. Bulbulian, A.M. Hollenbach, Inhalation of ultrafine and fine particulate matter disrupts systemic vascular function, Inhal. Toxicol. 19 (2007) 133–140.
[11] Q. Sun, A. Wang, X. Jin, A. Natanzon, D. Duquaine, R.D. Brook, J.G. Aguinaldo, Z.A. Fayad, V. Fuster, M. Lippmann, L.C. Chen, S. Rajagopalan, Long-term air pollution exposure and acceleration of atherosclerosis and vascular inflammation in an animal model, J. Am. Med. Assoc. 294 (2005) 3003–3010.
[12] T. Suwa, J.C. Hogg, K.B. Quinlan, A. Ohgami, R. Vincent, S.F. van Eeden, Particulate air pollution induces progression of atherosclerosis, J. Am. Coll. Cardiol. 39 (2002) 935–942.
[13] L. Calderón-Garcidueñas, A. Mora-Tiscareño, E. Ontiveros, G. Gómez-Garza, G. Barragán-Mejía, J. Broadway, S. Chapman, G. Valencia-Salazar, V. Jewells, R.R. Maronpot, C. Henriquez-Roldan, B. Pérez-Guillé, R. Torres-Jardón, L. Herritt, D. Brooks, N. Osnaya-Brizuela, M.E. Monroy, A. Gonzalez-Maciel, R. Reynoso-Robles, R. Villarreal-Calderon, A.C. Solt, R.W. Engle, Air pollution, cognitive deficits and brain abnormalities: a pilot study with children and dogs, Brain Cogn. 68 (2008) 117–127.
[14] M.L. Block, L. Calderón-Garcidueñas, Air pollution: mechanisms of neuroinflammation and CNS disease, Trends Neurosci. 32 (2009) 506–516.
[15] E.M. Thomson, P. Kumarathasan, L.C. Garciduenas, R. Vincent, Air pollution alters brain and pituitary endothelin-1 and inducible nitric oxide synthase gene expression, Environ. Res. 105 (2007) 224–233.
[16] J.W.C. Leung, S.S.M. Chung, S.K. Chung, Endothelial endothelin-1 overexpression using receptor tyrosine kinase tie-1 promoter leads to more severe vascular permeability and blood brain barrier breakdown after transient middle cerebral artery occlusion, Brain Res. 1266 (2009) 121–129.
[17] M. Weis, J.P. Cooke, Cardiac allograft vasculopathy and dysregulation of the NO synthase pathway, Arterioscler. Thromb. Vasc. Biol. 23 (2003) 567–575.
[18] A.W. de Souza, H. Ataíde Mariz, E. Torres Reis Neto, A.E. Diniz Arraes, N.P. da Silva, E.I. Sato, Risk factors for cardiovascular disease and endothelin-1 levels in Takayasu arteritis patients, Clin. Rheumatol. 28 (2009) 379–383.
[19] G. del Zoppo, I. Ginis, J.M. Hallenbeck, C. Iadecola, X. Wang, G.Z. Feurstein, Inflammation and stroke: putative role for cytokines, adhesion molecules and iNOS in brain response to ischemia, Brain Pathol. 585 (2000) 95–112.
[20] Z. Zheng, M.A. Yenari, Post-ischemic inflammation: molecular mechanisms and therapeutic implications, Neurol. Res. 26 (2004) 884–892.
[21] S.Z. Zhang, Y.L. Yue, X.Y. Yu, G.L. He, Distribution of ambient particle concentration in Taiyuan, J. Hyg. Res. 37 (2008) 331.
[22] M.E. Gerlofs-Nijland, A.J. Boere, D.L. Leseman, Effects of particulate matter on the pulmonary and vascular system: time course in spontaneously hypertensive rats, Part. Fibre Toxicol. 2 (2005) 2.
[23] J. Seagrave, J.D. McDonald, E. Bedrick, Lung toxicity of ambient particulate matter from southeastern U.S. sites with different contributing sources: relationships between composition and effects, Environ. Health Perspect. 114 (2006) 1387–1393.
[24] G.E. Hatch, R. Slade, E. Boykin, P.C. Hu, F.J. Miller, D.E. Gardener, Correlation of effects of inhaled versus intratracheally injected metals on susceptibility to respiratory infection in mice, Am. Rev. Respir. Dis. 124 (1981) 167–173.
[25] R. Bai, L. Zhang, Y. Liu, L. Meng, L. Wang, Y. Wu, W. Li, C. Ge, L. Le Guyader, C. Chen, Pulmonary responses to printer toner particles in mice after intratracheal instillation, Toxicol. Lett. 199 (2010) 288–300.
[26] B. Brunekreef, S.T. Holgate, Air pollution and health, Lancet 360 (2002) 1233–1242.
[27] N.L. Mills, K. Donaldson, P.W. Hadoke, N.A. Boon, W. MacNee, F.R. Cassee, T. Sandström, A. Blomberg, D.E. Newby, Adverse cardiovascular effects of air pollution, Nat. Clin. Pract. Cardiovasc. Med. 6 (2009) 36–44.
[28] S.M.J. MohanKumar, A. Campbell, M. Block, B. Veronesi, Particulate matter, oxidative stress and neurotoxicity, Neurotoxicology 29 (2008) 479–488.
[29] J. Bauersachs, A. Bouloumie, D. Fraccarollo, K. Hu, R. Busse, G. Ertl, Endothelial dysfunction in chronic myocardial infarction despite increased vascular endothelial nitric oxide synthase and soluble guanylate cyclase expression: role of enhanced vascular superoxide production, Circulation 100 (1999) 292–298.
[30] A.M. Shah, P.A. MacCarthy, Paracrine and autocrine effects of nitric oxide on myocardial function, Pharmacol. Ther. 86 (2000) 49–86.
[31] S. Verma, T.J. Anderson, The ten most commonly asked questions about endothelial function in cardiology, Cardiol. Rev. 9 (2001) 250–252.
[32] M.W. MacCumber, C.A. Ross, S.H. Snyder, Endothelin in brain: receptors, mitogenesis, and biosynthesis in glial cells, Proc. Natl. Acad. Sci. U.S.A. 87 (1990) 2359–2363.
[33] S. Yoshimoto, Y. Ishizaki, H. Kurihara, T. Sasaki, M. Yoshizumi, M. Yanagisawa, Y. Yazaki, T. Masaki, K. Takakura, S. Murota, Cerebral microvessel endothelium is producing endothelin, Brain Res. 508 (1990) 283–285.
[34] H. Monnerie, S. Esquenazi, S. Shashidhara, P.D. Le Roux, β-Amyloid-induced reactive astrocytes display altered ability to support dendrite and axon growth from mouse cerebral cortical neurons in vitro, Neurol. Res. 27 (2005) 525–532.
[35] J.P. O'Callaghan, K. Sriram, Glial fibrillary acidic protein and related glial proteins as biomarkers of neurotoxicity, Expert Opin. Drug Saf. 4 (2005) 433–442.
[36] F. Dong, X. Zhang, L.E. Wold, Q. Ren, Z. Zhang, J. Ren, Endothelin-1 enhances oxidative stress, cell proliferation and reduces apoptosis in human umbilical vein endothelial cells: role of ET(B) receptor, NADPH oxidase and caveolin-1, Br. J. Pharmacol. 145 (2005) 323–333.

[37] J.I. Herseth, V.V. Volden, P.E. Schwarze, M. Låg, M. Refsnes, IL-1beta differently involved in IL-8 and FGF-2 release in crystalline silica-treated lung cell co-cultures, Part. Fibre Toxicol. 5 (2008) 16.
[38] G. Stoll, S. Jander, M. Schroeter, Inflammation and glial responses in ischemic brain lesions, Prog. Neurobiol. 56 (1998) 149–171.
[39] A. Tailor, N. Granger, Role of adhesion molecules in vascular regulation and damage, Curr. Hypertens. Rep. 2 (2000) 78–83.
[40] M.O. Hengartner, The biochemistry of apoptosis, Nature 407 (2000) 770–776.
[41] Y. Wang, G.S. Zhuang, A.H. Tang, The ion chemistry and the source of PM2.5 aerosol in Beijing, Atmos. Environ. 39 (2005) 3771–3784.
[42] G. Liu, Z. Niu, D. Van Niekerk, J. Xue, L. Zheng, Polycyclic aromatic hydrocarbons (PAHs) from coal combustion: emissions, analysis, and toxicology, Rev. Environ. Contam. Toxicol. 192 (2008) 1–28.
[43] P. Danihelka, Coal combustion and heavy metals pollution, Proc. Annu. Int. Pittsburgh Coal Conf. 13 (1996) 1067–1072.
[44] Y. Chen, G. Zhi, Y. Feng, Measurements of emission factors for primary carbonaceous particles from residential raw-coal combustion in China, Geophys. Res. Lett. 33 (2006) L20815, doi:10.1029/2006GLO26966.
[45] E. Tamagawa, S.F. van Eeden, Impaired lung function and risk for stroke: role of the systemic inflammation response, Chest 130 (2006) 1631–1633.
[46] D.L. Laskin, D.E. Heck, J.D. Laskin, Role of inflammatory cytokines and nitric oxide in hepatic and pulmonary toxicity, Toxicol. Lett. 102–103 (1998) 289–293.
[47] S.F. van Eeden, W.C. Tan, T. Suwa, H. Mukae, T. Terashima, T. Fujii, D. Qui, R. Vincent, J.C. Hogg, Cytokines involved in the systemic inflammatory response induced by exposure to particulate matter air pollutants (PM(10)), Am. J. Respir. Crit. Care Med. 164 (2001) 826–830.
[48] S.F. van Eeden, A. Yeung, K. Quinlam, J.C. Hogg, Systemic response to ambient particulate matter: relevance to chronic obstructive pulmonary disease, Proc. Am. Thorac. Soc. 2 (2005) 61–67.
[49] A. Ericsson, C. Liu, R.P. Hart, P.E. Sawchenko, Type 1 interleukin-1 receptor in the rat brain: distribution, regulation, and relationship to sites of IL-1-induced cellular activation, J. Comp. Neurol. 361 (1995) 681–698.
[50] S. Nadeau, S. Rivest, Effects of circulating tumor necrosis factor on the neuronal activity and expression of the genes encoding the tumor necrosis factor receptors (p55 and p75) in the rat brain: a view from the blood–brain barrier, Neuroscience 93 (1999) 1449–1464.
[51] S. Rivest, How circulating cytokines trigger the neural circuits that control the hypothalamic-pituitary-adrenal axis, Psychoneuroendocrinology 26 (2001) 761–788.
[52] R.A. Borgerding, S. Murphy, Expression of inducible nitric oxide synthase in cerebral endothelial cells is regulated by cytokine-activated astrocytes, J. Neurochem. 65 (1995) 1342–1347.
[53] R.A. Shafer, S. Murphy, Activated astrocytes induce nitric oxide synthase-2 in cerebral endothelium via tumor necrosis factor alpha, Glia 21 (1997) 370–379.
[54] D.C. Dorman, K.A. Brenneman, A.M. McElveen, S.E. Lynch, K.C. Roberts, B.A. Wong, Olfactory transport: a direct route of delivery of inhaled manganese phosphate to the rat brain, J. Toxicol. Environ. Health A 65 (2002) 1493–1511.
[55] G. Oberdorster, Z. Sharp, V. Atudorei, A. Elder, R. Gelein, W. Kreyling, C. Cox, Translocation of inhaled ultrafine particles to the brain, Inhal. Toxicol. 16 (2004) 437–445.
[56] J. Lewis, G. Bench, O. Myers, B. Tinner, W. Staines, E. Barr, K.K. Divine, W. Barrington, J. Karlsson, Trigeminal uptake and clearance of inhaled manganese chloride in rats and mice, Neurotoxicology 26 (2005) 113–123.